Ecohydrology

What does airborne LiDAR really measure in upland ecosystems?

Journal:	*Ecohydrology*
Manuscript ID:	ECO-13-0201.R1
Wiley - Manuscript type:	Research Article
Date Submitted by the Author:	20-Jun-2014
Complete List of Authors:	Luscombe, David; University of Exeter, Geography, College of Life and Environmental Sciences Anderson, Karen; University of Exeter, Environment and Sustainability Institute Gatis, Naomi; University of Exeter, Geography, College of Life and Environmental Sciences Wetherelt, Andy; University of Exeter, Camborne School of Mines Grand-Clement, Emilie; University of Exeter, Geography, College of Life and Environmental Sciences Brazier, Richard; University of Exeter, Geography, College of Life and Environmental Sciences
Keywords:	LiDAR, Peatlands, Terrestrial Laser Scanning, Ecosystem services

What does airborne LiDAR really measure in upland ecosystems?

June 2014

David J Luscombe[1], Karen Anderson[2], Naomi Gatis[1], Andy Wetherelt[3], Emilie Grand-Clement[1] and Richard E Brazier[1]

Corresponding author: David J Luscombe, Email:d.j.luscombe@exeter.ac.uk, Tel:07748968462

[1] Geography, CLES, University of Exeter, Amory Building, Rennes Drive, Exeter, Devon EX4 4RG

[2] Environment and Sustainability Institute, University of Exeter, Cornwall Campus, Treliever Road, Penryn, Cornwall, TR10 9EZ

[3] Camborne School of Mines, University of Exeter (Cornwall Campus), Tremough Penryn, Cornwall, TR10 9EZ

ABSTRACT

Airborne laser scanning systems (LiDAR) are very well suited to the study of landscape and vegetation structure over large extents. Spatially distributed measurements describing the 3D character of landscape surfaces and vegetation architecture can be used to understand eco-geomorphic and ecohydrological processes, and this is particularly pertinent in peatlands given the increasing recognition that these landscapes provide a variety of ecosystem services (water provision, flood mitigation, carbon sequestration). In using LiDAR data for monitoring peatlands, it is important to understand how well peatland surface structures (with fine length scales) can be described. Our approach integrates two laser scanning technologies, namely Terrestrial Laser Scanning and airborne LiDAR surveys, to assess how effective airborne LiDAR is at measuring these fine scale microtopographic ecohydrological structures. By combining airborne and terrestrial laser scanning, we demonstrate an improved spatial understanding of the signal measured by the airborne LiDAR. Critically, results demonstrate that LiDAR DSMs are subject to specific errors related to short-sward ecosystem structure, causing the vegetation canopy height and surface-drainage network depth to be underestimated. TLS is shown to be effective at describing these structures over small extents, allowing the information content and accuracy of airborne LiDAR to be understood and quantified more appropriately. These findings have important implications for the appropriate degree of confidence ecohydrologists can apply to such data when using them as a surrogate for field measurements. They also illustrate the need to couple LiDAR data with ground validation data in order to improve assessment of ecohydrological function in such landscapes.

Keywords: LiDAR, Terrestrial Laser Scanning, DSM, Uncertainty, Peatlands, Uplands, Ecohydrology, Ecosystem services, Exmoor, UK.

INTRODUCTION

There is a new monitoring imperative for peatlands as global policy recognises the importance of these ecosystems in tackling climate change, water management objectives and biodiversity conservation (Bain et al. 2011; Grand-Clement et al. 2013). Spatially distributed measurements from airborne laser scanning systems such as Airborne Light Detection And Ranging (LiDAR), are useful for describing the three dimensional structure of landscape surfaces and vegetation (Emanuel 2013; Hutton and Brazier 2012; Mitchell et al. 2012; Rango et al. 2000; Zimble et al. 2003), and there is considerable evidence that such data provide valuable information on ecohydrological and eco-geomorphic processes in peatlands (Korpela et al. 2009; Anderson & Bennie 2010). In addition, landscape and ecosystem structure have long been recognised as important controls on peatland function (Moore and Bellamy 1974; Barber 1981). More recently Belyea and Clymo (2001) have explored the link between microtopography and peat formation and the *eco*hydrology of mires, leading to the contemporary understanding of links between microtopography and ecohydrological functioning summarised by Holden (2005) and Lindsay (2010).

The use of laser scanning techniques in peatlands could permit the quantification of how peatland structure and function change through time, leading to a dynamic understanding of landscape-scale ecohydrological behaviour (Fisher et al. 2009; Lane and D'Amico 2010; Turnbull et al. 2008). However, progress towards this in an operational sense is limited by our understanding of what the LiDAR signal actually represents in real terms – e.g. can LiDAR deliver robust measurements of both the short-sward canopy and/or the landscape surface? Spatially distributed information on both of these factors is needed because many temperate peatlands are dominated by low sward vegetation (Drewitt and Manley 1997) with structurally subtle micro-topographic features (Kincey and Challis 2009; Lindsay 2010): both of which impart significant effects on the ecohydrological functioning of peatlands (Holden et al. 2004).

Small shifts in ecological structure or drainage pattern may, for example, elicit major shifts in the hydrological response of the system.

LiDAR technologies use a precisely timed laser pulse and measure the return signal to capture accurate altimetry measurements of the Earth's surface, over large spatial extents. When analysing LiDAR datasets at landscape scales, there is often an assumption that the data are directly representative of the 3-D habitat structure (e.g. forest canopy) or the true ground surface (Jones et al. 2008; Kincey and Challis 2009). For example, LiDAR-derived digital surface models (DSMs) are often used to calculate hillshade products (Barbier et al. 2011; Kincey and Challis 2009), canopy height models for forestry (Zimble et al. 2003), or used to support numerical models of wetness, surface roughness or surface flows. (Beven 2012; Beven and Freer 2001; Jones et al. 2008). Previous work (Ivanov 1981; Taylor 1983) highlights the need for accurate representation of peatland surface flows in particular, to characterise peatland systems effectively. As a result, this approach can provide a powerful means of separating ecological and topographic structures (Hutton and Brazier 2012; Hinsley et al. 2002; Vierling et al. 2008; Chassereau et al. 2011; Clawges et al. 2008; Horning et al. 2010). However, in using these data it is important to note that the applicability of LiDAR is always constrained by the spatial resolution of the processed LiDAR surface (i.e. the resolution of the DSM) and the spatial support (or footprint) of the laser beam itself (Fisher and Tate 2006). Datasets derived from airborne LiDAR are, therefore, subject to implicit (but often unquantified) uncertainty (Aguilar et al. 2010).

Whilst we acknowledge that LiDAR datasets offer an as yet unparalleled ability to understand landscape structure and function (Korpela et al. 2009; Vierling et al. 2008; Zimble et al. 2003; Evans and Lindsay 2010; Rango et al. 2000), herein we stress the need to better quantify the spatial (*x, y*) and vertical (*z*) uncertainty in such data. This would permit an improved interpretation of LiDAR products describing the biotic and abiotic structure of peatlands. One way of approaching the problem is to integrate data from other laser scanning technologies operating at finer spatial resolutions (Danson, F. M. et al. 2007), in order to validate the information content of the LiDAR. Here we combine data from a terrestrial laser scanner (TLS) with airborne LiDAR surveys of an upland peatland system in the UK to test the following hypotheses:

1. TLS data can be used to validate the information content of a LiDAR DSM in an upland peatland context, thereby allowing improved spatial characterisation of ecohydrological structures such as above-ground biomass and surface-flow pathways.
2. Airborne LiDAR data allow the discrimination of different ecohydrologically relevant vegetation communities in peatlands.
3. Airborne LiDAR data are capable of detecting the presence and position of anthropogenic landscape features such as drains and archaeological remains which may alter hydrological function in peatlands.

METHODS

Airborne LiDAR data acquisition and initial processing

Airborne LiDAR data were collected by the Environment Agency Geomatics Group (EAGG) (www.geomatics-group.co.uk) in May 2009 at a 0.5 m spatial resolution in the horizontal plane. Two headwater catchments within degraded upland peatland areas in Exmoor National Park, UK were selected to include a wide range of drainage ditch morphology, slope morphology, aspect and vegetation composition. The location of the watershed of these upland catchments (known locally as 'Aclands' [SS 733,384] and 'Spooners' [SS 776,374]) is shown in Figure 1. LiDAR data supplied by EAGG were provided as a 'first return' dataset (0.3 m diameter footprint) and fitted to an even grid of 0.5 × 0.5 m by the data supplier. These data were then processed within a Geographical Information System (GIS; ArcGIS version 9.3.1) to produce a DSM with a cell size equal to 0.5 m. The LiDAR dataset was checked for accuracy at 5 separate locations by Geomatics group, using a differential Global Positioning System (DGPS) survey. These ground truth data indicated an average systematic error (or bias) of + 0.0004 m and an average random bias of ± 0.047 m in elevation. The combined RMSE for these data was 0.029 m which was well within the product specification of 0.15 m (personal communication to the author from the EAGG, 2012).

#Figure 1 approximately here#

TLS data collection and processing

Ground-based, terrestrial laser scanning (TLS) systems utilise a similar approach to airborne LiDAR, but typically cover smaller extents at finer spatial resolutions. Unlike airborne LiDAR, TLS systems are deployed from one or more fixed locations on the ground surface and have proven useful in providing data describing spatial structural proxies for peatland ecohydrological condition (Anderson et al. 2009; Anderson et al. 2010). Here, TLS data were collected *in situ* using a Leica Geosystems HDS 3000 scanner at the Spooners headwater catchment, in January 2011. The scanner collected ca. 1800 points per second spaced at 0.003 m, with a resultant dataset of > 7.5×10^6 points over a spatial extent of 4.2×10^3 m^2 in this example. The instrument uses a green laser (wavelength 532 nm), with a beam size of < 6 mm, positional accuracy of < 6 mm and range accuracy of < 4 mm (at a range of < 50 m; Anderson et al. 2009). Data were collected from multiple viewpoints above the peatland surface (Figure 2), and were registered into a single point cloud for each site following the method of Anderson et al (2009). Highly visible static stakes were deployed within the survey area to facilitate point-cloud registration; their positions were known to an accuracy of 0.005 m following a DGPS survey. To ensure the scanner had sufficient height above the peatland surface and thus an appropriate angle of incidence to the ground, a flat-bedded tracked vehicle was deployed at each of the scan locations providing a stable elevated platform of a consistent height (ca. 2 m) throughout the survey. The site selected for the survey included three artificial drainage ditches measuring approximately 0.3 m × 0.3 m in cross section and was dominated by vegetation typical of the majority of the hill slope area within the catchment. The vegetation included a mixed soft rush (*Juncus effusus*) and purple moor grass (*Molinia caerulea*) dominated sward in which the *M. caerulea* grew in tussock form.

#Figure 2 approximately here#

A DGPS survey was also used to provide validation transects through the TLS scan areas to provide an independent means of verifying the information content and accuracy of both the TLS and LiDAR datasets during subsequent stages of the analysis. DGPS survey points were taken at 3 – 5 m intervals along a transect and at each location the position of the ground surface and the top of the nearest dense grass tussock structures were recorded, creating pairs of measurements along the transect. The accuracy of the DGPS measurements was ± 0.5 cm in *x, y* and ± 2 cm in *z*. The registered TLS point cloud data were imported into Arc GIS 9.3.1. A 10 m × 10 m area of interest (AOI) was chosen in an area of dense point cloud coverage and to include a known surface drainage feature.

Subsequent processing aimed to extract the vertical extent of the top of canopy and ground surface respectively. The highest and lowest z values within a moving window filter of 0.05 m×0.05 m were extracted for the AOI extent and then processed into a 0.01 m discontinuous horizontal grid. A 1 cm grid resolution was chosen to preserve the fine scale variability of the point cloud in the surface generated. To prevent over-representation of outlying cloud points, the resultant data were then aggregated to a grid with a cell size matching the 0.05 m × 0.05 m filter used. Finally, a continuous 0.01 m grid was then interpolated from these data, using the ordinary spherical Kriging method to match the resolution of the discontinuous grid surface. The result was two products - (a) 'TLSmax' - the maximum vertical extent (assumed top of canopy) and (b) 'TLSmin' – the minimum vertical extent (assumed ground surface). For the next stage of processing the same AOI was extracted from the airborne LiDAR data so that the two datasets could be combined.

Combined TLS and LiDAR data analysis

In order to address hypothesis one, DSMs generated from both LiDAR and TLS data were compared to understand their information content. A new dataset was derived from the TLSmax, TLSmin and LiDAR data to describe their spatial relationship in three dimensions. Both TLSmax and TLSmin surfaces were classified as either above the height of the LiDAR DSM or below the LiDAR DSM. These classified data were then overlaid on top of a simple hillshade model of both TLSmax and TLSmin to enhance the visual comparison. The percentage of the TLSmax and TLSmin surfaces above and below the LiDAR DSM was then calculated. A transect through both DSMs was plotted alongside the raw TLS point cloud to provide a cross-sectional representation of the relationship between the datasets.

LiDAR analysis to discriminate vegetation and anthropogenic structures

To address hypotheses two and three, a model describing the high frequency spatial variation in LiDAR *z* (height) was needed. Data were filtered using a 'low pass' moving window (11 × 11 pixel neighbourhood) in ERDAS Imagine 2011, resulting in a 'smoothed' surface. These data were subtracted from the original DSM to derive a detrended surface. The low pass window of 11 × 11 pixels was selected to be larger than the maximum patch size of the canopy and microtopographic structure without degrading the signature of the underlying topography. The detrended surface enabled discontinuities in the data to be extracted and classified. For example, step changes that could indicate human activity (e.g. drainage ditches or archaeological remains) (Newman 2010), or areas where the DSM structure changed as a function of shifts in vegetation structure or composition.

Detrended data derived from the LiDAR DSM were used to identify the *x, y* position of microtopographic sinks within the peatland (e.g. tussock/hollow topography or drains). Within the detrended data, sinks were identified automatically by selecting pixels with a height (*z*) threshold of -0.11 m. As the *z* values in the detrended data represent the height difference from a smoothed surface, negative values highlighted the microtopographic sinks in the landscape, such as drainage features. A *z* threshold of -11 cm was chosen on the basis of expert field knowledge of this catchment (this was the minimum depth in the model that could highlight known anthropogenic drainage networks). To analyse the resultant layer further, data were processed to calculate the density of the classified pixels in two dimensional (*x, y*) space. Step changes in the density of these pixels were then used to classify the sinks as being either drainage features or vegetation characteristic of wet flushes.

Comparison with hydrological models and vegetation maps

Finally, high-resolution aerial photography (2 cm spatial resolution, collected April 2012) was used for the whole Aclands catchment to define the spatial distribution of six distinct vegetation communities based on the species assemblages outlined by Backshall et al. (2001) (wet and dry *Molinia caerulea*, *Juncus* flush, minerotrophic grassland, wet bog, and wet heath). These communities were differentiated using visual changes in canopy structure that were present in the imagery used. These vegetation categories were then manually digitised in order to support interpretation of the RS data analysis under hypothesis two. Although subjective, this technique identified abrupt changes in vegetation at a finer spatial resolution (0.02 m) than the LiDAR DSM (0.5 m) and was therefore considered sufficiently accurate.

In addition, to support hypothesis three, the raw LiDAR DSM was interrogated with an overland flow accumulation modelling algorithm based on the methods described in Jenson and Domingue (1988). This methodology includes the removal of topographic sinks to ensure flow connectivity. The resulting stream network was then classified using the Strahler stream order hierarchy (Strahler 1957). The Jenson and Domingue (1988) model assumes all precipitation becomes runoff and none is lost to interception or groundwater. Although this approach is hydrologically simplified, overland flow is often the predominant discharge from upland peatland systems (Charman 2002; Holden 2005) and therefore this simplicity is scientifically justified and appropriate to describe the hypothetical functioning of surface drainage features in the catchment.

RESULTS

Hypothesis one: results of combined TLS and LiDAR analysis

To address hypothesis one, the difference between topographic patterns from the TLS and LiDAR data was evaluated. The comparison of TLSmin and TLSmax surfaces to the LiDAR DSM (Figure 3) help to quantify the spatial relationship of TLS and LiDAR data in three dimensions. Most strikingly, the patterning evident in figure 3 illustrates that the linear surface drain feature (highlighted) in the TLSmin surface is almost entirely below the plane of the LiDAR DSM. In the TLSmax surface (3a) almost all of the areas that are lower than the LiDAR DSM correspond with gaps in the vegetation canopy, and are common to both 3a and 3b. These locations are visible as shared surface elements and low points in the landscape by both TLSmax and TLSmin. The results in table 1 illustrate that 45% of the TLSmin layer is below the plane of the LiDAR DSM. In contrast, for TLSmax over 87% of the surface is above the plane of the LiDAR DSM. Therefore if TLS data are considered to be ‘correct’, LiDAR data overestimate the level of the ground surface in 45% of the AOI and underestimate the vegetation canopy in 87% of the AOI.

#Figure 3 approximately here#

#Table 1 approximately here#

Figure 4 provides more detailed illustration of the relationship between these surfaces along an east – west cross section through the LiDAR and TLS derived DSMs within the AOI. The TLS point cloud exhibits significant vertical variation along this transect with an increased density toward the bottom of its range. The TLSmin surface has an overall trend similar to the LiDAR surface (illustrated in figure 5) although data are more variable than the LiDAR data, falling both above and below the LiDAR DSM in figure 4. Importantly, there is a region (annotated as Drainage Ditch in figure 4) that falls markedly below the plane of the LiDAR data but also corresponds with the position of a drainage ditch in the landscape. In contrast, the TLSmax surface demonstrates a level consistently above the plane of the LiDAR data both as discrete data (figure 4) and as an overall trend (figure5).

Along this transect, the TLSmax surface also exhibits areas of both high and low variation from the TLSmin surface. In addition, there are six discrete regions in which the TLSmin layer displays increased divergence from the plane of the LiDAR layer (figure 4). These regions also correspond with positions at which the TLSmax surface peaks and the density of the TLS point cloud noticeably decreases. Plotting DGPS points measuring the position of the dense tussock structures and the adjacent ground surface across an extended transect, permits a further test of how well the LiDAR data represents the ground surface (figure 6).

#Figure 4 approximately here#

#Figure 5 approximately here#

Data in figure 6 confirm that the LiDAR DSM is largely bounded by the surveyed ground surface and the vertical height of the dense tussock structure in this transect. Furthermore, at any DGPS point pair, the LiDAR surface appears skewed toward *either* the ground surface (DGPS tussock bottom) or the tussock tops, with no consistent bias.

#Figure 6 approximately here#

Hypotheses two and three: discrimination of vegetation and anthropogenic structures

The extraction of spatially distinct areas of microtopographic sinks from the detrended LiDAR DSM supports evaluation of both hypotheses 2 and 3. In this analysis, dense areas of microtopographic sinks do not fit the expected position of the discrete linear features known to be anthropogenic drainage features. Figure 7 illustrates the results of manually digitising dominant vegetation classes across the catchment (7a) from high-resolution aerial photography (7b) and comparing these with the dense areas of microtopographic sinks classified from detrended LiDAR data from (7c). Visual comparison of the images suggests that the large extents of wet *Molinia caerulea* and wet *Juncus spp.* dominated vegetation observed in the catchment are also captured by the LiDAR data as a complex surface characterised by a high density of microtopographic sinks. The contiguous area that is mapped as wet *Molinia caerulea* and wet *Juncus spp.* from aerial photography represents 15.9% of the catchment, versus 18.6% that the LiDAR classification delineates as dominated by vegetation and microtopography characteristic of flushed areas. The smaller (often linear) areas of *Juncus spp.* in the west of the catchment are however, not described well by the LiDAR classification.

#Figure 7 approximately here#

With respect to hypothesis three, figure 8a reveals that anthropogenic landscape features with constrained vertical variation (≥ -0.11 m) can also be identified and classified using the detrended LiDAR DSM, and the spatial extent of such features delineated and measured. The linear structure of surface drains is visible here as black pixels, alongside the dense areas of microtopographic sinks (blue pixels) used to delineate the flushed (wet *Molinia caerulea* and wet *Juncus spp dominated)* areas. The linear anthropogenic features extracted using these classifications appear discontinuous across the land surface. Indeed, when the LiDAR DSM is used as an input to simple overland flow routing algorithms (Fig 8b) the anthropogenic drainage features extracted (shown as blue lines) demonstrate only a weak control on these flow pathways (grey scale, darker colours representing higher order channels). Many higher order flow accumulation pathways also appear to function entirely independently of the mapped artificial drainage network outlined in blue (Fig 8b), in agreement with the disconnected nature of linear features extracted in fig 8b. The LiDAR data, whilst able to detect the 2D location of drainage ditches, does not therefore appear able to quantify whether or not they are continuous drainage features in the landscape.

#Figure 8 approximately here#

DISCUSSION

Moving beyond qualitative visual analysis of LiDAR data, such as simple hillshade models, is an essential step to quantify landscape scale ecohydrological functioning and the associated landscape services. Given this, understanding the accuracy with which LiDAR products are able to measure ecohydrologically-relevant structures in the uplands is critical if such analysis is to be considered representative of “real world” structure and subsequent function. This study has shown that while vegetation canopy height and drainage ditch depth are underestimated by airborne LiDAR DSMs, the aerial extent of these features can still be determined in a spatial context. The following sections discuss the various ramifications of these findings.

Vertical accuracy of LiDAR Data – combined LiDAR and TLS analysis

Hypothesis one explored how airborne LiDAR DSMs compare with TLS data, in relation to their abilities to capture structural information about vegetation and topography. Numerous researchers have alluded to the sources of error in a wide range of DSM’s (Fisher and Tate 2006; Li et al. 2011; Wise 2011). However, few authors propose solutions to resolve levels of error with respect to independent measurements (see Aguilar et al. 2010 and Hodgson and Bresnahan 2004 for notable exceptions). Herein, we illustrate that the TLSmax and TLSmin surfaces describe the maximum and minimum measured vertical extent of the vegetation canopy at a fine spatial resolution. Therefore, TLS data are extremely useful in describing the information content and error associated with airborne LiDAR data and its ability to describe spatial shifts in vegetation organisation. Data presented in figure 3 illustrate that the LiDAR DSM elevation values correlate with the TLSmin surface far more than they do with the TLSmax surface over the extent of the AOI (87% of TLSmax is above the plane of the LiDAR data). These results demonstrate that the LiDAR data most closely represent the ground surface and not the canopy structure. Furthermore, the highlighted surface drain feature (figure 3) is entirely below the plane of the LiDAR DSM in the AOI studied. Such underestimation of vegetation canopy heights and the depth of drainage features have important implications where LiDAR-derived structures are used as indicators of ecohydrological condition (Anderson et al. 2010), and as inputs to spatially distributed models (Beven, 2011).

More detailed analysis of the magnitude of vertical variation between the LiDAR and TLS layers (figures 4 and 5) also illustrated that the LiDAR DSM more closely represents a smoothed version of the ground surface (described by the TLSmin data) lacking microtopographic structure. Topographic features, such as the surface drainage network, are estimated in error in DSM data for the following reasons according to Fisher and Tate (2006):

- Variability in the accuracy, density and distribution of source data,
- Processing and interpolation
- Characteristics of the terrain surface being modelled.

In this case the LiDAR DSMs created provide one *x, y, z* coordinate for every 0.5 m cell, which is a relatively coarse resolution when compared with the scale of drainage ditch features (often they are only 0.3 m wide in these landscapes). In addition, the dense, low-sward vegetation tussocks disrupt the return of the laser pulse from the ground surface such that microtopographic depressions are not captured consistently, especially when tussock forming grasses occur within, or overhang, surface drainage pathways (as evident in figure 3). Therefore, in contrast to forested landscapes, where vegetation is typically less dense and more uniform in height (Vierling et al 2008), it is likely that LiDAR DSMs will always generate an uncertain representation of the ecosystem structure in short-sward ecosystems. In this example, the LiDAR DSM is biased towards the ground surface, as delineated by the TLSmin dataset, which lies consistently close to and above the trend line for the LiDAR DSM (figure 5).

To understand the specific effect of denser vegetation components on the LiDAR DSM, DGPS survey data were also compared with the LiDAR surface. Figure 6 illustrated that the LiDAR DSM data captured the ground surface *and* dense grass tussock centres reasonably well as a composite surface, with all points falling within the bounds created from the DGPS measurements. This additional data analysis suggests that the LiDAR DSM data represent both the ground surface and the denser components of the vegetation structure *only* and not the sward canopy structure. For an airborne product flown at an altitude of 800 – 1000m above ground level, this ability to approximate the range of tussock top-bottom values suggests some promise in using the LiDAR DSM in these low-sward landscapes to assess habitat structure (Anderson et al. 2010; Korpela et al. 2009; Vierling et al. 2008). However, these results highlight the necessity to evaluate the modelled LiDAR surface with finer resolution data prior to inference of ecohydrological structure. Indeed, where LiDAR data are used to provide metrics of habitat condition without three-dimensional validation of observed vegetation structures such as TLS (Kincey and Challis 2009; Korpela et al. 2009; Li et al. 2011; Streutker and Glenn 2006), the certainty with which we can use LiDAR data to understand the condition of these systems spatially is limited.

TLS data in isolation also provide a useful tool in the quantification of both the ecological and hydrological structure of these upland ecosystems over smaller extents. The technique presented here provides discrete layers which are useful in measuring vegetation canopy/biomass and the underlying surface structure. Whether used independently or in conjunction with airborne LiDAR, critical evaluation of TLS data is still necessary to ensure robust interpretation. For example, data presented here (figure 4) illustrate that at locations where the point cloud becomes sparse the TLSmin layer appears to offer a markedly poorer representation of the underlying ground surface. In agreement with wider studies using TLS (Anderson et al. 2009; Watt and Donoghue 2005), these findings highlight the difficulties of using TLS data to measure complex and fine-scaled vegetation structure in situ. In this case, the error is attributable to the method of data generation (Fisher and Tate 2006). i.e. vegetation canopy completely obscuring the ground from the laser or because the area is subject to shadowing in the point cloud. As such, this deviation of the TLSmin surface from the LiDAR DSM agrees with the LiDAR data predominantly describing a smoothed ground surface. However, these results illustrate that structural measurements from any platform, even at fine spatial scales, can be subject to the same sources of error in short sward ecosystem.

Discrimination of vegetation and anthropogenic structures

Although the preceding results and discussion demonstrate that LiDAR data underestimate both canopy height and drainage network volume, numerical interrogation of detrended LiDAR data has shown that spatial information on ecohydrologically relevant vegetation communities (hypothesis 2) and anthropogenic drainage features (hypothesis 3), can still be captured. Data in figure 7 confirm that the detrended LiDAR data can be used to effectively map the extent of flushed (i.e. wetter) vegetation communities. However, the preceding findings suggest that increased surface complexity used to delineate these areas is, in fact, a measurement of the change in the sub-canopy, highlighting microtopographic landforms associated with these waterlogged vegetation communities dominated by *Juncus* spp. and wet *Molinia caerulea* stands.

Features identified as anthropogenic peatland surface drainage in this analysis have been validated as being (largely) continuous and connected, following extensive fieldwork and GPS mapping of drainage features at these sites (figure 8). However, results in figure 8 suggest that they appear to be highly discontinuous features when detected by LiDAR. Under-representation of microtopographic structure in LiDAR DSMs (figure 4) explains why such drainage features extracted for the Aclands catchment in figure 8a appear to be discontinuous. Consequently, these features are shown to have only a limited influence on the flow paths modelled in the flow accumulation model illustrated in figure 8b, though in reality, they may be highly significant in controlling surface-flow networks. The extent to which such LiDAR data can be relied upon as good representations of microtopography (anthropogenic or otherwise) controlling ecohydrological function, is therefore subject to the same implicit error or uncertainty previously discussed (Jones et al. 2008). Where such data are used as inputs to numerical hydrological models in peatland landscapes (Rothwell et al. 2010), understanding such uncertainty in the representation of drainage structure is critical to ensure the spatial quality of model predictions.

Acknowledging the error and understanding the source of it in such data can also be advantageous to the ecohydrologist. Knowing the nature of the error and its magnitude makes airborne LiDAR data potentially far more powerful as inputs to ecohydrological modelling frameworks. For example, using numerical processing such as “growing” extracted features (Espindola et al. 2006) describing discontinuous drainage features and using these to modify DSM values (Li et al. 2011) may allow researchers to represent the connectivity of surface drainage structures in a modelled catchment more accurately. Subsequently, better predictions of both the spatial distribution of flow routing and resultant downstream hydrographs may result, in turn aiding the quantification of the associated ecohydrological landscape services (Grand-Clement et al. 2013). These data also highlight the value of a combined RS approach in confirming assumptions made from any one dataset. For example, cross validation of modelled surface wetness indices generated from LiDAR and TABI (airborne thermography data), (Luscombe et al. 2012) or LiDAR and near infra-red data (Harris and Bryant 2009) can be performed, enabling the observed ecohydrological patterning to be evaluated prior to integration into numerical modelling of the ecohydrological functioning.

CONCLUSION

This paper demonstrates that the spatially explicit measurements provided by LiDAR datasets are subject certain to specific errors, related to both the spatial resolution of the dataset and the interaction of laser ranging systems with short-sward landscapes. Results show that airborne LiDAR data underestimate vegetation canopy volume/height and the volume/depth of surface drainage networks, both of which are key spatial variables in understanding ecohydrological functioning at a landscape scale. Understanding this uncertainty improves the way in which these data can be used as numerical model inputs, and the confidence which researchers should place on these data when used as a surrogate for field measurements over a variety of disciplines and ecosystems. Furthermore, this work demonstrates that using TLS data, the canopy structure *can* be described at a fine spatial resolution and with greater precision than with LiDAR data, although over far smaller extents. These data illustrate the need to couple LiDAR data with fine spatial resolution altimetry data (i.e. TLS) and field measurements, to improve models of the ecosystem structure and describe the spatial attributes of the ecosystem at a scale that is appropriate to capture the ecohydrological functioning of the landscape.

References

Aguilar FJ, Mills JP, Delgado J, Aguilar MA, Negreiros JG, Perez JL. 2010. Modelling vertical error in LiDAR-derived digital elevation models. *ISPRS Journal of Photogrammetry and Remote Sensing* **65(1)** : 103-110.

Anderson K, Bennie J, Wetherelt A. 2009. Laser scanning of fine scale pattern along a hydrological gradient in a peatland ecosystem. *Landscape Ecology* **25(3)** : 477-492.

Anderson K, Bennie J, Milton EJ, Hughes PDM, Lindsay R, Meade R. 2010. Combining LiDAR And Ikonos Data For Eco-hydrological Classification Of An Ombrotrophic Peatland. *Journal of Environmental Quality*. **39(1)** : 260-273.

Backshall J, Manley J, Rebane M. 2001. *The Upland Management Handbook*. English Nature.

Bain CG, Bonn A, Stoneman R, Chapman S, Coupar A, Evans M, Gearey B, Howat M, Joosten H, Keenleyside C, Labadz J, Lindsay R, Littlewood N, Lunt P, Miller CJ, Moxey A, Orr H, Reed M, Smith P, Swales V, Thompson D.B.A, Thompson P.S, Van de Noort R, Wilson JD, Worrall F. 2011. *IUCN UK Commission of Inquiry on Peatlands*. IUCN UK Peatland Programme: Edinburgh.

Barber KE. 1981. *Peat Stratigraphy and Climatic Change*. Rotterdam : Balkema.

Barbier N, Proisy C, Vega C, Sabatier D, Couteron P. 2011. Bidirectional texture function of high resolution optical images of tropical forest: An approach using LiDAR hillshade simulations. *Remote Sensing of Environment* **115(1)** : 167-179.

Belyea LR, Clymo RS. 2001. Feedback control of the rate of peat formation. *Proceedings of the Royal Society of London: Biological Sciences* **268 :** 1315 - 1321.

Beven K. 2012. *Rainfall-Runoff Modelling, The Primer*. John Wiley & Sons Ltd: Chichester.

Beven K, Freer J. 2001. A dynamic TOPMODEL. *Hydrological Processes* **15(10)** : 1993-2011.

Charman D. 2002. *Peatlands and Environmental Change*. John Wiley & Sons Ltd: Chichester.

Chassereau JE, Bell JM, Torres R. 2011. A comparison of GPS and LiDAR salt marsh DEMs. *Earth Surface Processes and Landforms* **36(13)** : 1770-1775.

Clawges R, Vierling K, Vierling L, Rowell E. 2008. The use of airborne lidar to assess avian species diversity, density, and occurrence in a pine/aspen forest. *Remote Sensing of Environment* **112(5)** : 2064-2073.

Danson FM, Hetherington D, Morsdorf F, Koetz B, Allgower B. 2007. "Forest Canopy Gap Fraction From Terrestrial Laser Scanning." *Geoscience and Remote Sensing Letters*, IEEE **4(1)** : 157-160.

Drewitt AL, Manley VJ. 1997. *The vegetation of the mountains and moorlands of England*. English Nature Research Reports. English Nature, pp. 218.

Emanuel RE, Hazen AG, McGlynn BL, Jencso KG. 2013. Vegetation and topographic influences on the connectivity of shallow groundwater between hillslopes and streams. *Ecohydrology* **7** : 887-895. DOI: 10.1002/eco.1409

Espindola GM, Camara G, Reis IA, Bins LS, Monteiro AM. 2006. Parameter selection for region growing image segmentation algorithms using spatial autocorrelation. *International Journal of Remote Sensing* **27(14)** : 3035-3040.

Evans M, Lindsay J. 2010. High resolution quantification of gully erosion in upland peatlands at the landscape scale. *Earth Surface Processes and Landforms* **35(8)** : 876-886.

Fisher B, Turner RK, Morling P. 2009. Defining and classifying ecosystem services for decision making. *Ecological Economics* **68(3)** : 643-653.

Fisher PF, Tate NJ. 2006. Causes and consequences of error in digital elevation models. *Progress in Physical Geography* **30(4)** : 467-489.

Grand-Clement E, Anderson K, Smith D, Luscombe DJ, Gatis N, Ross M. Brazier RE. 2013. Evaluating ecosystem goods and services after restoration of marginal upland peatlands in South-West England. *Journal of Applied Ecology* **50(2) :** 324-334.

Harris A, Bryant RG. 2009. A multi-scale remote sensing approach for monitoring northern peatland hydrology: Present possibilities and future challenges. *Journal of Environmental Management* **90(7)** : 2178-2188.

Hinsley SA, Hill RA, Gaveau DLA, Bellamy PE. 2002. Quantifying woodland structure and habitat quality for birds using airborne laser scanning. *Functional Ecology* **16(6)** : 851-857.

Hodgson ME, Bresnahan P. 2004. Accuracy of airborne lidar-derived elevation: empirical assessment and error budget. *Photogrametric Engineering and Remote Sensing* **70(3)** : 331-340.

Holden J, Chapman PJ, Labadz JC. 2004. Artificial drainage of peatlands: hydrological and hydrochemical process and wetland restoration. *Progress in Physical Geography* **28(1)** : 95–123.

Holden, J. 2005. Peatland hydrology and carbon release: why small-scale process matters. *Philosophical Transactions of the Royal Society a-Mathematical Physical and Engineering Sciences* **363** : 2891-2913.

Horning N, Robinson JA, Sterling EJ, Turner W, Spector S (eds). 2010. *Remote Sensing for Ecology and Conservation*: *A Handbook of Techniques*. Oxford University Press: Oxford and New York.

Hutton C, Brazier RE. 2012. Quantifying riparian zone structure from airborne LiDAR: Vegetation filtering, anisotropic interpolation, and uncertainty propagation. *Journal of Hydrology* **442-443(0)** : 36-45.

Ivanov KE. 1981. *Water movement in mirelands*. Academic Press Inc: London.

Jenson SK, Domingue JO. 1988. Extracting topographic structure from digital elevation data for geographic information system analysis. *Photogrammetric Engineering and Remote Sensing* **54(11)** : 1593-1600.

Jones KL, Poole GC, O'Daniel SJ, Mertes LAK, Stanford JA. 2008. Surface hydrology of low-relief landscapes: Assessing surface water flow impedance using LIDAR-derived digital elevation models. *Remote Sensing of Environment* **112(11)** : 4148-4158.

Kincey M, Challis K. 2009. Monitoring fragile upland landscapes: The application of airborne lidar. *Journal for Nature Conservation* **18(2)** : 126-134.

Korpela I, Koskinen M, Vasander H, Holopainen M, Minkkinen K. 2009. Airborne small-footprint discrete-return LiDAR data in the assessment of boreal mire surface patterns, vegetation, and habitats. *Forest Ecology and Management* **258(7)** : 1549-1566.

Lane C, D'Amico E. 2010. calculating the ecosystem service of water storage in isolated wetlands using LiDAR in north central Florida, USA. *Wetlands* **30(5)** : 967-977.

Li S, MacMillan RA, Lobb DA, McConkey BG, Moulin A, Fraser WR. 2011. Lidar DEM error analyses and topographic depression identification in a hummocky landscape in the prairie region of Canada. *Geomorphology* **129(3-4)** : 263-275.

Lindsay R. 2010. *Peatbogs and Carbon*: A Critical Synthesis. University of East London: London.

Luscombe DJ, Anderson K, Grand-Clement E, Le-Feuvre N, Smith D, & Brazier RE. 2012. April. Assessing the ecohydrological status of a drained peatland: Combining thermal airborne imaging, laser scanning technologies and ground water monitoring. *EGU General Assembly Conference Abstracts* (Vol. 14, p. 740).

Mitchell PJ, Lane PNJ, Benyon RG. 2012. Capturing within catchment variation in evapotranspiration from montane forests using LiDAR canopy profiles with measured and modelled fluxes of water. *Ecohydrology* **5(6) :** 708-720.

Moore PD, Bellamy DJ. 1974. *Peatlands*. London : Elek Science.

Newman P. (2010). Domestic and industrial peat cutting on North-Western Dartmoor, Devonshire. An archaeological and historical investigation. In. South-West landscape Investigations reports, Dartmoor National Park.

Rango A, Chopping M, Ritchie J, Havstad K, Kustas W, Schmugge T. 2000. morphological characteristics of shrub coppice dunes in desert grasslands of southern new mexico derived from scanning LIDAR. *Remote Sensing of Environment* **74(1) :** 26-44.

Rothwell JJ, Lindsay JB, Evans MG, Allott THE. 2010. Modelling suspended sediment lead concentrations in contaminated peatland catchments using digital terrain analysis. *Ecological Engineering* **36(5) :** 623-630.

Strahler AN. 1957. Quantitative analysis of watershed geomorphology. *American Geophysical Union Transactions* **38(6) :** 912-920.

Streutker DR, Glenn NF. 2006. LiDAR measurement of sagebrush steppe vegetation heights. *Remote Sensing of Environment* **102(1)** : 135-145.

Taylor J. 1983. Peatlands of Great Britain and Ireland. In: *Mires: Swamp, Bog, Fen and Moor. 4B Regional Studies (Ecosystems of the World)* ed. Gore AJP. pp. 1-46. Elsevier Scientific: Amsterdam.

Turnbull L, Wainwright J, Brazier RE. 2008. A conceptual framework for understanding semi-arid land degradation: ecohydrological interactions across multiple-space and time scales. *Ecohydrology* **1(1)** : 23-34.

Vierling KT, Vierling LA, Gould WA, Martinuzzi S, Clawges RM. 2008. LiDAR: shedding new light on habitat characterization and modeling. *Frontiers in Ecology and the Environment* **6(2)** : 90-98.

Watt PJ, Donoghue DNM. 2005. Measuring forest structure with terrestrial laser scanning. *International Journal of Remote Sensing* **26(7)** : 1437-1446.

Wise S. 2011. Cross-validation as a means of investigating DEM interpolation error. *Computers & Geosciences* **37(8)** : 978-991.

Zimble DA, Evans DL, Carlson GC, Parker RC, Grado SC, Gerard PD. 2003. Characterizing vertical forest structure using small-footprint airborne LiDAR. *Remote Sensing of Environment* **87(2-3)** : 171-182.

Tables

Table 1, Percentage of the TLSmax and TLSmin layers that have z values above and below the plane of the LiDAR derived DSM.

Classification	TLS Max Surface	TLS Min Surface
% below LiDAR DSM	13	45
% above LiDAR DSM	87	55

Figure captions

Figure 1: a) and b) Location of Aclands and Spooners study catchments and c) the TLS study area within Spooners watershed defined from airborne LiDAR data. d) and e) illustrate the study area used for the TLS survey. d) Shows the scan locations and AOI overlaying an aerial photograph of the study area (Co-ordinates for upper left 51° 7'23.81"N, 3°45'2.76"W and bottom right 51° 7'21.69"N, 3°44'59.70"W). e) Shows the spatial extent of the TLS data collected as a grid, each dot representing one of > 7.5×10^6 data points.

Figure 2: TLS data capture locations and respective overlapping scan zones. The darker polygon within the station 4 scan region represents the area of greatest point cloud overlap as shown in figure 1e). The Area of Interest (AOI) is indicated, showing that it lies within the zone of maximal point-cloud overlap.

Figure 3: Hillshade models of both (a) TLSmax and (b) TLSmin Surfaces for the Area of Interest (AOI). Areas higher than the LiDAR DSM surface are overlain with black and those below the LiDAR DSM are overlain with white.

Figure 4: TLS and LiDAR topographic profiles extracted from the Studied AOI within Spooners Catchment. TLSmax and TLSmin represent the maximum and minimum vertical extent of the TLS data along this transect. Annotations highlight the position of the drainage ditch in the transect and an example of a location where TLSmin and LiDAR surfaces diverge as a result of a sparser point cloud density.

Figure 5: Modelled relationships (second order polynomial, N =1040 for TLSmax and TLSmin) describing the under-representation of the vegetation canopy (TLSmax) by LiDAR DSM data. Data are generated as trends of topographic profiles extracted in figure 4.

Figure 6: Alternate LiDAR topographic profile extracted from the wider TLS scan zone (figure 1) within Spooners catchment. DGPS Survey data describing the maximum and minimum vertical extent of dense vegetation components (tussocks) are included as paired measurements along the transect length.

Figure 7: Habitat mapping of Aclands Catchment. (a) Vegetation communities digitised from aerial imagery. (b) High resolution aerial photograph. (c) Flushed vegetation Area delineated from classified LiDAR data.

Figure 8: Mapping of surface drainage. (a) Data extracted from detrended LiDAR data (Aclands Catchment) and classified into surface drainage networks, whether natural or artificial (Black pixels) and rush dominated "flushed" zones (blue pixels). Pixels were classified using a threshold of pixel density. (b) A simple overland flow accumulation model with streams ordered using the Strahler classification (Strahler 1957) whereby stream size is classified according to a hierarchy of tributaries. A stream with no tributaries is 1st order; when two 1st order streams meet they subsequently form a 2nd order stream and so on. Only 4th to 9th order streams are displayed.

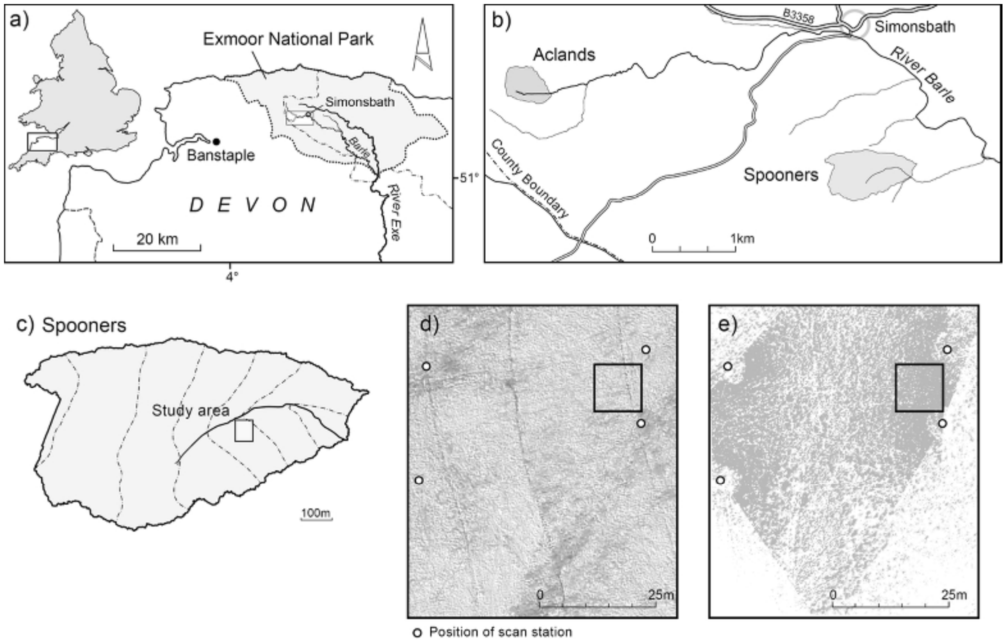

Figure 1: a) and b) Location of Aclands and Spooners study catchments and c) the TLS study area within Spooners watershed defined from airborne LiDAR data. d) and e) illustrate the study area used for the TLS survey. d) Shows the scan locations and AOI overlaying an aerial photograph of the study area (Co-ordinates for upper left 51° 7'23.81"N, 3°45'2.76"W and bottom right 51° 7'21.69"N, 3°44'59.70"W). e) Shows the spatial extent of the TLS data collected as a grid, each dot representing one of > 7.5 × 106 data points.
107x72mm (300 x 300 DPI)

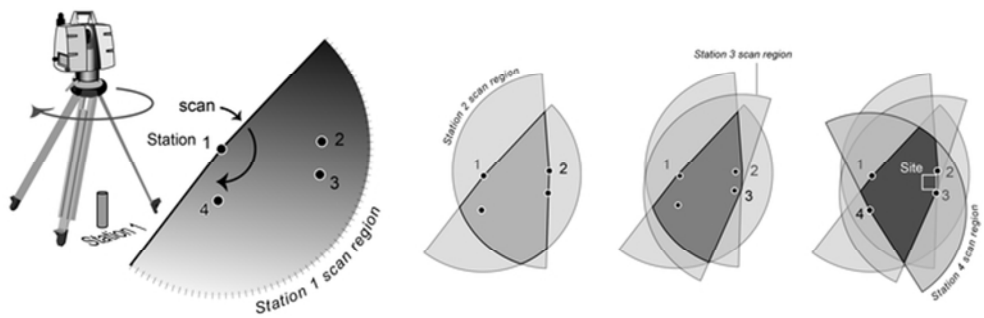

Figure 2: TLS data capture locations and respective overlapping scan zones. The darker polygon within the station 4 scan region represents the area of greatest point cloud overlap as shown in figure 1e). The Area of Interest (AOI) is indicated, showing that it lies within the zone of maximal point-cloud overlap.
57x20mm (300 x 300 DPI)

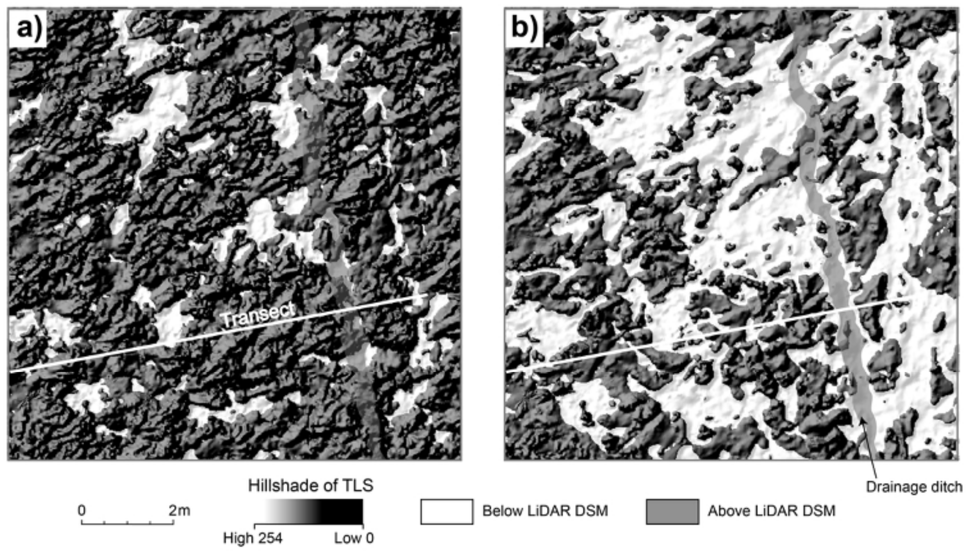

Figure 3: Hillshade models of both (a) TLSmax and (b) TLSmin Surfaces for the Area of Interest (AOI). Areas higher than the LiDAR DSM surface are overlain with black and those below the LiDAR DSM are overlain with white.
94x54mm (300 x 300 DPI)

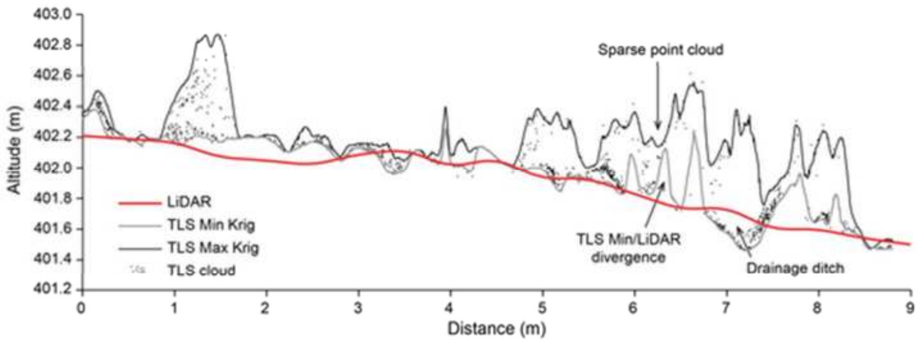

Figure 4: TLS and LiDAR topographic profiles extracted from the Studied AOI within Spooners Catchment. TLSmax and TLSmin represent the maximum and minimum vertical extent of the TLS data along this transect. Annotations highlight the position of the drainage ditch in the transect and an example of a location where TLSmin and LiDAR surfaces diverge as a result of a sparser point cloud density.
52x21mm (300 x 300 DPI)

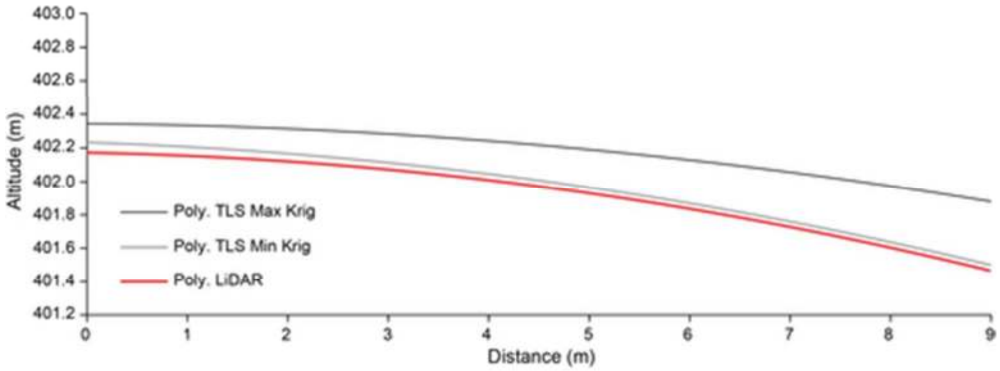

Figure 5: Modelled relationships (second order polynomial, N =1040 for TLSmax and TLSmin) describing the under-representation of the vegetation canopy (TLSmax) by LiDAR DSM data. Data are generated as trends of topographic profiles extracted in figure 4.
41x15mm (300 x 300 DPI)

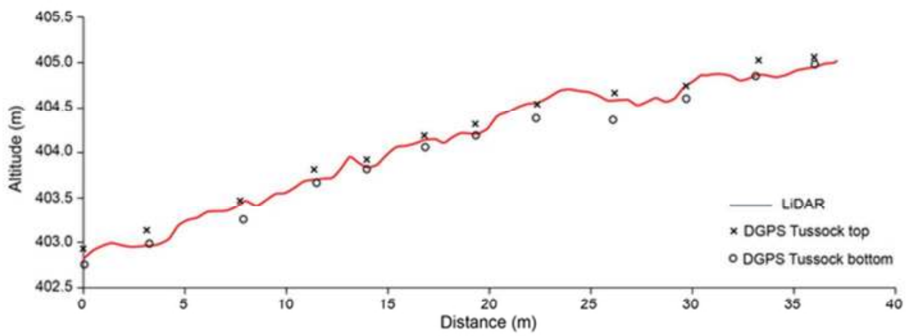

Figure 6: Alternate LiDAR topographic profile extracted from the wider TLS scan zone (figure 1) within Spooners catchment. DGPS Survey data describing the maximum and minimum vertical extent of dense vegetation components (tussocks) are included as paired measurements along the transect length.
58x27mm (300 x 300 DPI)

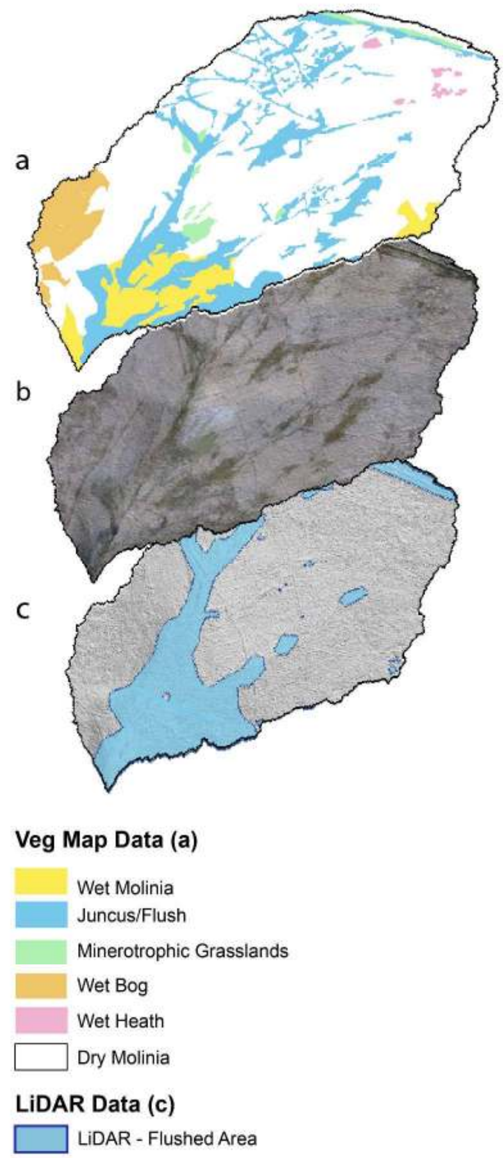

Figure 7: Habitat mapping of Aclands Catchment. (a) Vegetation communities digitised from aerial imagery. (b) High resolution aerial photograph. (c) Flushed vegetation Area delineated from classified LiDAR data.
184x415mm (300 x 300 DPI)

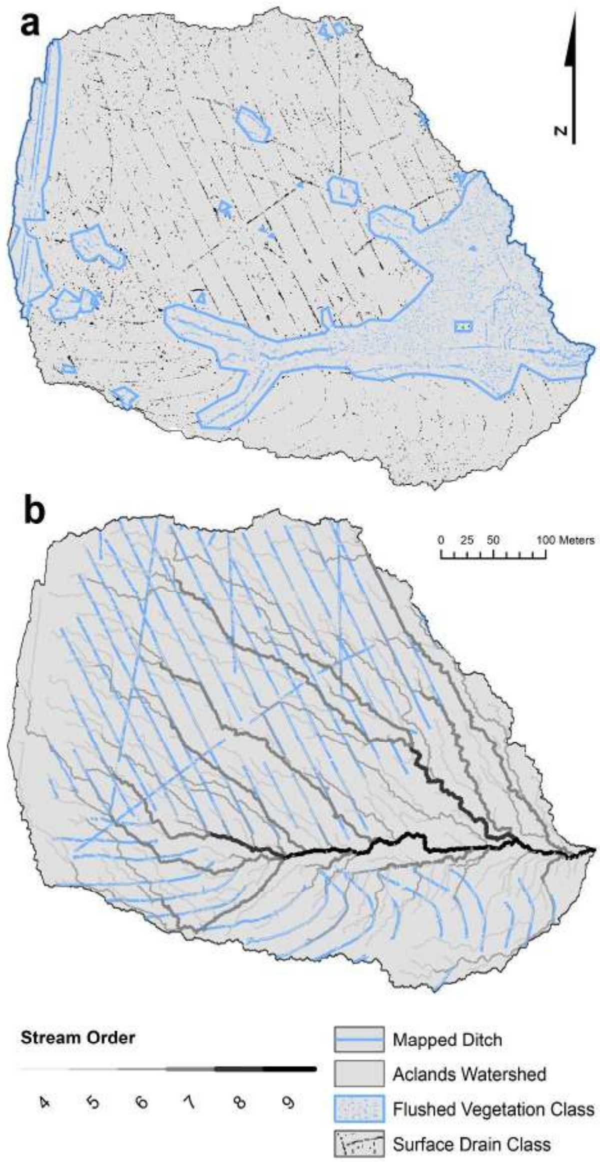

Figure 8: Mapping of surface drainage. (a) Data extracted from detrended LiDAR data (Aclands Catchment) and classified into surface drainage networks, whether natural or artificial (Black pixels) and rush dominated "flushed" zones (blue pixels). Pixels were classified using a threshold of pixel density. (b) A simple overland flow accumulation model with streams ordered using the Strahler classification (Strahler 1957) whereby stream size is classified according to a hierarchy of tributaries. A stream with no tributaries is 1st order; when two 1st order streams meet they subsequently form a 2nd order stream and so on. Only 4th to 9th order streams are displayed.
146x279mm (600 x 600 DPI)